

High-Resolution Coherent Raman Spectroscopy of Vibrons in Solid Parahydrogen

著者	Kuroda K., Koreeda A., Takayanagi S., Suzuki M., Hakuta K.
journal or publication title	Physical Review. B
volume	67
number	18
page range	184303
year	2003
URL	http://hdl.handle.net/10097/52612

doi: 10.1103/PhysRevB.67.184303

High-resolution coherent Raman spectroscopy of vibrons in solid parahydrogen

K. Kuroda, A. Koreeda,* S. Takayanagi, M. Suzuki, and K. Hakuta

Department of Applied Physics and Chemistry, University of Electro-Communications, Chofu, Tokyo 182-8585, Japan
and CREST, Japan Science and Technology Corporation (JST), Chofu, Tokyo 182-8585, Japan

(Received 11 October 2002; revised manuscript received 27 March 2003; published 30 May 2003)

Coherent Raman spectroscopy is carried out for the $Q_1(0)$ vibron of solid parahydrogen crystal with a spectral resolution better than 1 MHz. The Raman spectrum is measured for the temperature from 4.2 to 13 K under constant molecular density condition. We show that the temperature dependence of the Raman spectrum should be quantitatively described via the interaction between vibrons and thermal acoustic phonons through a two-phonon scattering process. We also investigate the effect of molecular density on the Raman shift and obtain the hopping interaction strength for the vibron band.

DOI: 10.1103/PhysRevB.67.184303

PACS number(s): 33.20.Ea, 42.65.Dr, 67.80.-s

I. INTRODUCTION

Solid hydrogen is the simplest molecular crystal; it consists of H_2 molecules and is known as one of the quantum crystals.^{1,2} It has been attracting much interest in various fields of physics, such as low-temperature physics, thermodynamics, and spectroscopy. One unique feature of solid hydrogen is that the intermolecular binding potential energy is so small compared to the vibrational and rotational energies of an H_2 molecule that the H_2 molecules making up the crystal can freely rotate and vibrate at each crystal site. Accordingly, there have been many high-resolution spectroscopic approaches to date using various vibrational and rotational transitions.^{3,4}

Furthermore, it has been demonstrated recently that the unique nature of solid hydrogen may have a special significance in optical physics. New types of nonlinear optical processes, such as self-induced phasematching, arbitrary and efficient parametric sideband generation even for incoherent fluorescence light, etc., are explored through the vibrational Raman transition $Q_1(0)(v=1-0, J=0-0)$ for parahydrogen.⁸ Among the spectral transitions of solid hydrogen, the $Q_1(0)$ transition is one of the purest, and detailed laser spectroscopies have been carried out by Oka and collaborators. Momose *et al.* showed that this transition reveals a very narrow spectral width of 6 MHz half width at half maximum (HWHM) at a temperature around 5 K.⁵ Kerr *et al.* measured the Raman transition using the Condon modulation method and discussed the mechanism of spectral shift and broadening.⁶ However, in order to establish a concrete basis for solid hydrogen as a nonlinear optical medium, it is essential to conduct much more detailed spectroscopies.

In the present work, we report on coherent Raman spectroscopy for the $Q_1(0)$ vibrational transition with a spectral resolution better than 1 MHz. We measure systematically the temperature dependence of the Raman spectra for the temperature range from 4.2 K to 13 K under a constant volume (constant molecular density) condition. We show that the temperature dependencies for both the Raman frequency and width are quantitatively explained through the interaction between the vibrational excitation (vibron) and acoustic phonon. We investigate also the effect of molecular density on the Raman shift and obtain the hopping interaction strength for the vibron band.

II. $Q_1(0)$ VIBRON RAMAN TRANSITION

Figure 1 illustrates an energy level diagram for the $Q_1(0)$ Raman transition in solid hydrogen. By incorporating the hopping interaction between the molecules through dispersive interaction, the vibrational state $v=1, J=0$ of solid hydrogen may well be described by a Bloch wave (exciton), termed vibron.² As illustrated, the vibron band spreads around the band origin, a free-molecule energy, with a width of 8ε , where ε is hopping interaction strength. The lowest edge of the vibron band locates at an energy 6ε lower than the band origin. On the other hand, in terms of the ground vibrational state ($v=0, J=0$) which does not have any degeneracy, it does not show the band structure and can be treated effectively by a single Bloch wave state of $\mathbf{k}=0$. Because of this single state nature of the ground state, the Raman transition from the ground state selectively picks up vibrons with $\mathbf{k}=0$ that locate at the lowest edge of the band.

III. EXPERIMENT

Solid parahydrogen crystal was prepared in a cell using the liquid-phase growing method.⁹ Liquid parahydrogen was

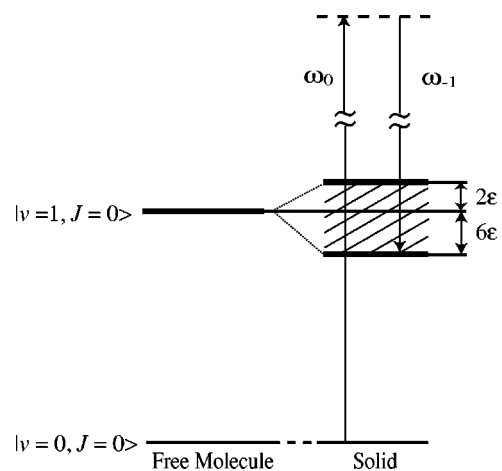


FIG. 1. Schematic diagram of the $Q_1(0)(v=1-0, J=0-0)$ vibron Raman transition. The Raman transition from the ground state picks up the bottom edge of the vibron band of $\mathbf{k}=0$ that locates below the band origin by 6ε , where ε denotes the hopping interaction strength of the vibron band.

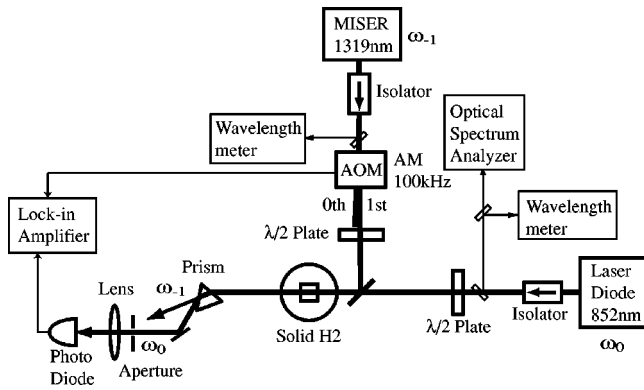


FIG. 2. Block diagram of the coherent Raman spectroscopy. The pump laser is a cw-YAG laser (MISER) at 1319 nm, and the probe laser is an external-cavity diode laser at 852 nm. The Raman resonance spectrum is measured by tuning the probe laser frequency. The pump beam is chopped at 100 kHz with an acousto-optic modulator (AOM).

obtained by converting from normal hydrogen using iron-oxide catalyst at 14 K, just above the melting point. The cell was a cylindrical shape and was made of stainless steel, 1 cm long and 1 cm in diameter. Optical sapphire windows were in place at both ends of the cell. The crystal grew from a copper seed-spot about 0.1 mm in diameter at the bottom of the cell. The temperatures of the cell and the seed-spot were kept at 15 and 14 K, respectively. The liquid hydrogen was pressurized during the crystal growth. The pressure was feedback-controlled to maintain a constant value using a computer in the range from 24 to 32 atm. The crystal grew to fill the whole cell in about 1 h; the cell temperature was then slowly lowered to 4.2 K. Thus, we prepared a completely transparent parahydrogen crystal without any visible cracks at 4.2 K. In order to check the residual orthohydrogen density, we measured an infrared orthohydrogen transition $Q_1(1)$ ($v = 1 - 0$, $J = 1 - 1$) at a wavelength of $2.4 \mu\text{m}$ using an FT spectrometer (Bomem DA8). The orthohydrogen concentration was estimated from the integrated intensity of the infrared absorption. The concentration was lower than 0.1% for all the crystals used for the measurements.

Figure 2 illustrates an experimental diagram for the coherent Raman spectroscopy. We used a pump and probe scheme; we observed the Raman transition by measuring an absorption spectrum for probe laser radiation by scanning its frequency around ω_0 under a pump laser radiation in Stokes side at ω_{-1} (see Fig. 1). We used two cw single-frequency lasers for the pump and probe beams; a monolithic YAG laser at 1319 nm (MISER, Lightwave Electronics, 126–1319) was used as the pump radiation source, and an external-cavity laser diode at 852 nm as the probe radiation source. Frequency stabilities of both lasers were estimated to be less than 200 kHz. The two laser beams were adjusted to the same linear polarization, coaxially overlapped, and loosely focused on the parahydrogen crystal. The wavelength of each laser was simultaneously measured by a wavelength meter (Burleigh, WA-1500) with an accuracy of ± 30 MHz. Incident powers for the pump and probe beams were typically 40 and 20 mW, respectively. The pump beam was

chopped at a frequency of 100 kHz using an acousto-optic modulator. The probe beam was separated from the pump beam with a prism, detected by a photodiode, lock-in amplified, and displayed and stored with a computer. In terms of the overall specifications of this Raman spectrometer, the spectral resolution was estimated to be better than 1 MHz, and the accuracy of Raman-frequency measurement was estimated to be ± 30 MHz.

We measured systematically the temperature dependence of the Raman spectra of solid hydrogen for the temperature range from 4.2 K to 13 K under a constant molecular density condition. We should note here that this constant molecular density condition is a key feature in the present experiments. Generally, in measuring the temperature dependencies of a solid sample, one serious problem is the thermal expansion/shrinkage of the sample which might change its molecular density, leading to some ambiguities in the theoretical interpretation of the results. By the present method, however, we had no ambiguity from the thermal expansion/shrinkage of the sample crystal, because the solid hydrogen crystal was grown to fully occupy a stainless-steel cell whose thermal expansion/shrinkage should be negligible for the temperature range of the measurements. Thus, we can measure the temperature dependencies under a constant volume condition, i.e., constant molecular density condition. Furthermore, we can change the molecular density of the sample crystal by controlling the applied pressure during the crystal growth. We estimated the molecular density of the crystals using the systematic experimental results for solid hydrogen for the molar volume¹⁰ and for the solidification curves.¹¹ The molecular density ρ of a crystal grown at 28 atm was estimated to be $8.68 \times 10^{-2} \text{ g/cm}^3$, and the molecular density change $\Delta\rho$ for a pressure change of ± 4 atm around 28 atm was estimated to be $\pm 0.013 \times 10^{-2} \text{ g/cm}^3$; that is, the relative density change $\Delta\rho/\rho$ was $\pm 1.5 \times 10^{-3}$ for the pressure change of ± 4 atm around 28 atm. We also estimated the $|\Delta\rho/\rho|$ value using an experimental equation of state for solid hydrogen,¹² which led to a slightly larger value of 1.8×10^{-3} .

IV. RESULTS AND DISCUSSION

The $Q_1(0)$ Raman spectra were measured for the temperature range from 4.2 to 13 K for crystals prepared under three different pressure conditions (32, 28, and 24 atm). Figure 3 displays a series of spectra obtained by changing the temperature for a crystal grown under a pressure of 32 atm. It is readily seen that, by raising the temperature, the Raman shift moves to the higher frequency side and the Raman width becomes broader with weaker peak intensity. We carefully checked the observed spectral profiles and found that they were all well reproduced by Lorentzian profiles and that the integrated intensity of the profile was preserved for a series of measurements. In the inset of the figure, we exhibit a spectral profile measured at 5.7 K on an enlarged scale. Black circles denote the measured points and a solid curve denotes a Lorentzian fitted curve with an HWHM of 5 MHz. Note that the instrumental resolution did not impose any restriction on the measurements. Note also that the effects of

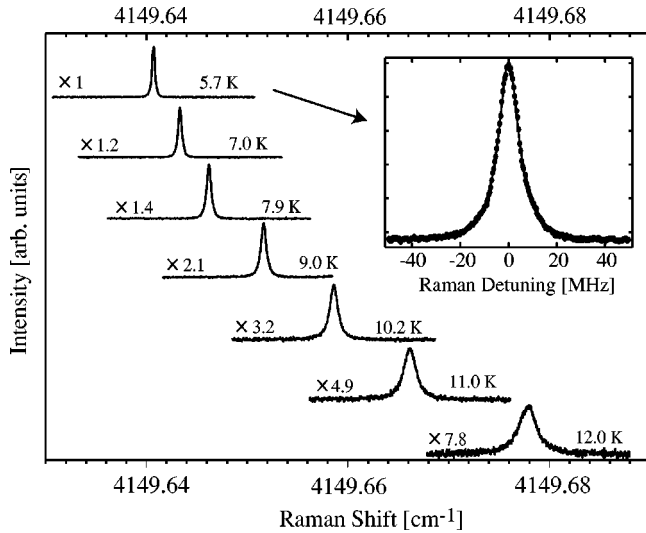


FIG. 3. Raman spectrum measured by changing the temperature for a crystal grown at 32 atm. The vertical scaling for each trace should be magnified by the factor denoted for each trace. The inset shows the Raman spectral profile at 5.7 K. Black circles denote the observed profile. The solid curve is a Lorentzian fitted profile with an HWHM of 5 MHz.

crystal inhomogeneity for the Raman profile are extremely small, much smaller than 5 MHz.

A. TEMPERATURE DEPENDENCE

The Raman shift and width for two crystals grown under pressure of 32 and 24 atm were plotted versus temperature and are displayed in Figs. 4(a) and 4(b). We expressed the observed Raman shift and width as $\nu = \nu_0 + \Delta\nu(T)$ and $\Gamma = \Gamma_0 + \Delta\Gamma(T)$, respectively. It is seen that the Raman shift moves down in parallel with the pressure increase, while the Raman width does not show the pressure effect clearly. We fitted the observed $\Delta\nu$ and $\Delta\Gamma$ by T^7 and found that they are well reproduced by the T^4 and T^7 dependencies, respectively [see the inset of Figs. 4(a) and 4(b)]. As discussed by McCumber and his colleagues for ionic impurities in molecular crystals, the temperature dependencies by T^4 and T^7 are typical behaviors for spectral lines embedded in a thermal acoustic phonon bath.^{13,14} The mechanism of the interaction is a two-phonon-scattering process. When a thermal phonon is described as the Debye phonon and the phonon frequency is much smaller than the spectral transition frequency, the expressions for $\Delta\nu$ and $\Delta\Gamma$ due to the two phonon scattering may be written as^{13,14}

$$\Delta\nu(T) = \alpha \left(\frac{T}{T_D} \right)^4 \int_0^{T_D/T} \frac{x^3}{e^x - 1} dx,$$

$$\Delta\Gamma(T) = \beta \left(\frac{T}{T_D} \right)^7 \int_0^{T_D/T} \frac{x^6 e^x}{(e^x - 1)^2} dx.$$

Here, T_D denotes Debye temperature, which was fixed to 100 K.¹⁵ The expressions mean that $\Delta\nu$ and $\Delta\Gamma$ are proportional to total phonon energy and to its square, respectively,

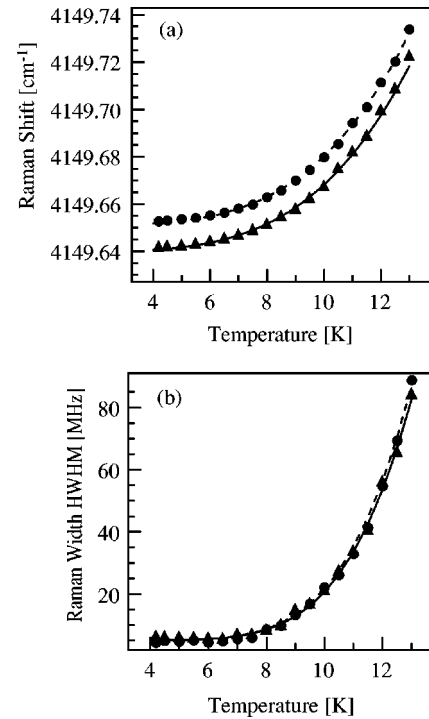


FIG. 4. Temperature dependencies for Raman shift (a) and width (b) for crystals grown under two different pressure conditions of 24 and 32 atm. Observed values for crystals grown at 24 and 32 atm are denoted by black circles and black triangles, respectively. Dashed and solid curves are least-squares-fitted curves for crystals grown at 24 and 32 atm, respectively.

and consequently that the effective parameters α and β may be proportional to the molecular density and its square, respectively. It should be mentioned here that since the present temperature range is much lower than the Debye temperature, the effect of the integrals on the temperature dependence appears only slightly for temperatures higher than 10 K and essential temperature dependencies are expressed as T^4 and T^7 for the Raman shift and width, respectively. We fitted the measured dependencies with the above expressions using the least-mean-squares method. The fitted curves are drawn in Figs. 4(a) and 4(b), showing very good agreement with the observed plots. This agreement clearly demonstrates that the temperature dependence is due to the interaction between vibron and acoustic phonon via two phonon scattering. Parameters ν_0 , α , Γ_0 , and β for the three crystals were obtained as listed in Table I. We have thus attributed the origin of the temperature dependencies to the vibron-phonon interaction, but in order to clarify the physical meaning of the effective parameters α and β , the vibron-phonon interaction must be formulated theoretically. Development of this theory is now in progress, and the details will be published elsewhere.

Related to this is the work by Kerr *et al.*⁶ They measured the temperature dependence of the $Q_1(0)$ vibron transition for both spectral position and width. One difference of their experiments from ours is that their crystal was grown by the gas phase growth method in a cell with an open space, which inevitably induces thermal expansion/shrinkage via tempera-

TABLE I. Obtained parameters for $Q_1(0)$ vibron Raman transition of solid hydrogen for three crystals grown under different pressure conditions. Crystals A, B, and C were grown at pressures of 24, 28, and 32 atm, respectively. Number in parenthesis is the least-squares-fitted uncertainty in the last digit of each parameter.

	Crystal A	Crystal B	Crystal C
ν_0 (cm $^{-1}$)	4149.654(1)	4149.648(1)	4149.642(1)
α (cm $^{-1}$)	61(4)	60(4)	59(4)
Γ_0 (MHz)	5.6(5)	4.9(5)	4.2(5)
β ($\times 10^4$ MHz)	42(3)	39(3)	39(3)

ture change. They discussed the mechanism of the temperature dependence in the context of molecular density change. Regarding the spectral position, they observed a temperature dependence of $T^{4.096}$. Although the behavior was almost consistent with our results, it was slightly steeper. This slight difference can be reasonably understood as being due to the shift of the $Q_1(0)$ vibron frequency to a higher frequency side in the high-temperature range, which may be expected through the volume expansion of the crystal that lowers the molecular density [see Fig. 4(a)]. Regarding the spectral widths, those measured by Kerr *et al.* were in the range broader than 100 MHz HWHM, and their temperature dependence was not simple enough to be fitted by T^η . We suspect that their broad spectral width might have been mainly due to the crystal inhomogeneity, and that this inhomogeneity might have spoiled the chance to obtain quantitative temperature dependence for the spectral width.

One could expect some effects on vibron shift and width from other freedoms of solid hydrogen, such as molecular rotation or anharmonic lattice vibration due to the quantum crystal nature. However, we did not observe any deviation from the simple Debye phonon interaction model. We are confident that these results are quite reasonable for the present measurements carried out for the temperature range from 4 to 13 K. Regarding the rotational motion, since we are dealing with $Q_1(0)(v=1-0, J=0-0)$, no rotational excitation is involved in the transition, and the effect of rotational motion should be negligible. Moreover, rotational motion should not affect the temperature dependence, since the lowest excited rotational state is located 354 cm $^{-1}$ higher than the ground $J=0$ level, which is too large compared to the thermal energy in the present experiments. Regarding nature of the quantum crystal, the lattice vibration of solid hydrogen deviates from the simple harmonic oscillator model in principle, but such effects might not be observable for a temperature range higher than 4 K; they might be observable only at very low temperatures of the mK region, since a critical parameter of the quantum tunneling motion might be very small at about 10 kHz.⁷

B. MOLECULAR DENSITY DEPENDENCE

As shown in Table I, concerning the pressure (molecular density) dependence of the parameters α and β , the values do not show any observable change outside of the experimental uncertainties with the present small density change of

$\Delta\rho/\rho \approx \pm 1.5 \times 10^{-3}$. Regarding parameter Γ_0 , it shows a slight tendency to become larger with decreasing density out of the experimental uncertainties. This tendency might not be due to intrinsic density-effects, since the lower density may result in a weaker vibron-phonon interaction leading to narrower spectral width, which should have an opposite tendency to that observed. We speculate that the observed tendency would be due to the crystal inhomogeneity, which might become larger for crystals grown under lower pressure conditions.

Regarding the dependence of ν_0 , we observed a systematic change versus applied pressure outside of experimental ambiguities. The observed pressure shift may be understood as being due to the shift of the lowest edge of the vibron band due to the change of molecular density. Since the lowest band edge position is directly related to the hopping interaction strength ε for the vibron band (see Fig. 1), and furthermore since the hopping interaction is originated from the dispersive interaction which is proportional to R^{-6} where R is intermolecular distance, the hopping strength ε can be expressed as $\varepsilon \propto \rho^2$. The observed behaviors can thus be explained. Conversely, using the relation $\varepsilon \propto \rho^2$ one can estimate the hopping interaction strength from the observed pressure dependence. By differentiating ε by ρ , the following relation can be obtained:

$$\varepsilon \approx \frac{1}{2} \rho \frac{\Delta\varepsilon}{\Delta\rho} \approx \frac{1}{12} \left(\frac{\Delta\rho}{\rho} \right)^{-1} \Delta\nu_0,$$

where ρ , $\Delta\rho$, and $\Delta\nu_0$ are molecular density, molecular density change, and frequency shift of ν_0 value by the density change, respectively. Thus, using the ν_0 values in Table I and the $\Delta\rho/\rho$ value for the pressure change of 4 atm, we were able to obtain the hopping interaction strength. Since the $\Delta\rho/\rho$ value has an ambiguity as discussed in Sec. III, we obtained the ε value using the two $\Delta\rho/\rho$ values. Assuming $|\Delta\rho/\rho| \approx 1.5 \times 10^{-3}$, we obtained a value $\varepsilon \approx 0.33 \pm 0.06$ cm $^{-1}$. We also obtained another value $\varepsilon \approx 0.27 \pm 0.06$ cm $^{-1}$ assuming $|\Delta\rho/\rho| \approx 1.8 \times 10^{-3}$. Here, the error was due to the uncertainty of the Raman shift measurements. Although the obtained values are slightly smaller than the theoretical value 0.4 cm $^{-1}$ determined by Van Kranendonk,¹⁶ the correspondence between experiment and theory is reasonably good.

V. CONCLUSIONS

In conclusion, we have measured the Raman spectrum of the $Q_1(0)$ vibron transition of solid parahydrogen with a spectral resolution better than 1 MHz under a constant molecular density condition. The Raman spectrum was systematically measured by changing the temperature for crystals with different molecular density. We have shown that the temperature dependence of this spectrum should be quantitatively described through the interaction between vibron and thermal acoustic phonon via a two-phonon-scattering process. It has also been shown that the inhomogeneity of the solid hydrogen crystal was extremely small, the inhomogeneous width might be much less than 5 MHz. This may

provide a special benefit in optical physics for designing various nonlinear optical processes. We have determined the hopping interaction strength for the vibron band via the molecular density dependence for the Raman spectrum.

ACKNOWLEDGMENTS

The authors thank Fam Le Kien and M. Katsuragawa for helpful discussions.

*Present address: Department of Physics, Tohoku University, Sendai, Japan

¹I. F. Silvera, *Rev. Mod. Phys.* **52**, 393 (1980).

²J. Van Kranendonk, *Solid Hydrogen* (Plenum, New York, 1983).

³T. Oka, *Annu. Rev. Phys. Chem.* **44**, 299 (1993).

⁴D. P. Weliky, T. J. Byers, K. E. Kerr, T. Momose, R. M. Dickson, and T. Oka, *Appl. Phys. B: Lasers Opt.* **59**, 265 (1994).

⁵T. Momose, D. P. Weliky, and T. Oka, *J. Mol. Spectrosc.* **153**, 760 (1992).

⁶K. E. Kerr, T. Momose, D. P. Weliky, C. M. Gabrys, and T. Oka, *Phys. Rev. Lett.* **72**, 3957 (1994).

⁷J. M. Delrieu and N. S. Sullivan, *Phys. Rev. B* **23**, 3197 (1981).

⁸K. Hakuta, M. Suzuki, M. Katsuragawa, and J. Z. Li, *Phys. Rev. Lett.* **79**, 209 (1997); J. Q. Liang, M. Katsuragawa, Fam Le Kien, and K. Hakuta, *ibid.* **85**, 2474 (2000); M. Katsuragawa, J. Q. Liang, Fam Le Kien, and K. Hakuta, *Phys. Rev. A* **65**, 025801

(2002).

⁹M. Suzuki, M. Katsuragawa, R. S. D. Sihombing, J. Z. Li, and K. Hakuta, *J. Low Temp. Phys.* **111**, 463 (1998).

¹⁰R. F. Dwyer, G. A. Cook, O. E. Berwaldt, and H. E. Nevins, *J. Chem. Phys.* **43**, 801 (1965).

¹¹N. G. Bereznyak and A. A. Sheinina, *Sov. J. Low Temp. Phys.* **6**, 608 (1980).

¹²A. Driessen and I. F. Silvera, *J. Low Temp. Phys.* **54**, 361 (1984).

¹³D. E. McCumber and M. D. Sturge, *J. Appl. Phys.* **34**, 1682 (1963).

¹⁴G. F. Imbusch, W. M. Yen, A. L. Shawlow, D. E. McCumber, and M. D. Sturge, *Phys. Rev.* **133**, A1029 (1964).

¹⁵P. C. Souers, *Hydrogen Properties for Fusion Energy* (University of California Press, Berkeley, 1986), pp. 99–101.

¹⁶J. Van Kranendonk, *Can. J. Phys.* **38**, 240 (1960).